Formation of novel thermoplastic composites using bicomponent nonwovens as a precursor

Mehmet Dasdemir · Benoit Maze ·
Nagendra Anantharamaiah · Behnam Pourdeyhimi

Abstract This study focuses on a novel technique to produce thermoplastic composites directly from bicomponent nonwovens without using any resins or binders. Conceptually, the structure of the bicomponent fibers making up these nonwovens already mimics the fiber–matrix structure of fiber reinforced composites. Using this approach, we successfully produced isotropic thermoplastic composites with polymer combinations of polyethylene terephthalate/polyethylene (PET/PE), polyamide-6/polyethylene (PA6/PE), polyamide-6/polypropylene (PA6/PP), and PP/PE. The effects of processing temperature, fiber volume fraction, and thickness of the preform on the formation and structure of the nonwoven composites were discussed. Processing temperatures of 130 and 165 °C for PE and PP matrices, respectively, resulted in intact composite structures with fewer defects, for fiber volume fraction values of up to 51%. Moreover, an insight into the changes on the fine structure of the bicomponent fibers after processing was provided to better explain the mechanics behind the process. It is hypothesized that the composite fabrication process can result in annealing and increases the degree of crystallinity and melting temperature of polymers by thickening lamellae and/or removing imperfections. One of the other outcomes of this study is to establish what combination of mechanical properties (tensile and impact) nonwoven composites can offer. Our results showed that compared to glass mat reinforced thermoplastic composites, these novel isotropic nonwoven composites offer high specific strength (97 MPa/g cm^{-3} for PA6/PE), very high strain to failure (152% for PP/PE), and superior impact strength (147 kJ/m^2 for PA6/PP) which can be desirable in many critical applications.

Introduction

Fiber reinforced composites are engineered materials that combine complementary properties of two constituents, fiber and matrix, to create a synergy on the overall properties. They can be separated into two groups according to the type of the matrix resin used. These are thermosets and thermoplastics. Even though thermoset resins are dominant in the composite market, there is a great impetus to use thermoplastics instead of thermosets. This is due to the fact that using thermosets in composite applications brings some drawbacks such as limited shelf time, comparatively higher processing costs and longer production time. Additionally, fracture toughness and damage tolerance of the composites can be greatly improved when thermoset matrices such as epoxies, unsaturated polyesters and vinyl esters were replaced with thermoplastics [1]. One of the other advantages of using thermoplastic materials in composite application is the ability to reprocess (reshape) and use it in a post-consumer application [2].

Conventional thermoplastic composite fabrication techniques are pultrusion and injection molding. These techniques can be used for short-fiber reinforced thermoplastics such as glass fiber reinforced composites. For long fibers, thermoplastic composites are made by wetting out the reinforcement components (in the form of aligned fiber, tape, and woven fabric) with polymer melt. The methods of making these composites require several steps including fiber formation, fabric or tape construction, and preparation of polymer melt, wetting, and drying. The main challenge in

M. Dasdemir · B. Maze (✉) · N. Anantharamaiah ·
B. Pourdeyhimi
The Nonwovens Institute, North Carolina State University,
Raleigh, NC, USA
e-mail: bmaze@ncsu.edu

current methods is to combine two distinct materials. This is due to the fact that the polymer melt has to follow long flow paths through the fibrous reinforcement. Therefore, impregnation by the matrix polymer and formation of defects (voids) in the structure are the main drawbacks of conventional thermoplastic composite fabrication techniques.

Matrix-less composites

A new concept of thermoplastic composite fabrication was first introduced in 1975 by Capiati and Porter [3]. In this approach, fiber component has aligned and extended chains; therefore, it has thermodynamically more stable crystals and higher melting point than conventionally crystallized matrix polymer. Thus, the difference in melting points between these two chemically identical components can be utilized to obtain a single polymer thermoplastic composite. Capiati and Porter [3] particularly studied all polyethylene composite and observed a partial melting of the fiber surface and a transcrystalline region at the interface. To evaluate the interfacial shear strength they performed single fiber pull-out test and found a high interfacial strength which was granted by the epitaxial bonding between two components.

Single polymer composites also known as self-reinforced or all-polymer or matrix-less composites then gained much attention due to the fact that they can provide good interfacial adhesion and enhanced recyclability. Several techniques have been developed: film stacking [4, 5], hot compaction [6–9], solution impregnation [10], wet powder impregnation [11], and co-extrusion [12–14]. Among these techniques, film stacking, hot compaction, and recently co-extrusion are the most popular due to the advantages such as strong fiber–matrix interface and high delamination resistance they can provide.

In the film stacking technique, polymer films with a lower melting point than the reinforcement fibers are placed in between preforms. Upon heating, these films melt and form the matrix. Even though interlayer films can improve delamination strength and allow a wide processing temperature window, penetration of polymer melt through fibers can still be problematic [4].

Hot compaction technique was first introduced in 1993 by Ward and his research team [6]. In this technique, a small fraction of the surface of each oriented fiber is melted by carefully controlling the temperature. At the same time, with the help of pressure, the molten polymer flows and fills the gap between remaining reinforcement fibers. Upon cooling, molten polymer epitaxially crystallizes on the initial fibers and forms the matrix phase. Initial research on the hot compaction was mostly done on melt spun polyethylene (PE) fibers [6, 15, 16]. After successful experimentation with melt spun PE, their research was extended to other highly and partially oriented thermoplastic fibers:

polyethylene terephthalate (PET) [17], polypropylene (PP) [18–20], gel spun PE [9], and polyamide 6.6 (PA6.6) [21]. These fibers were either unidirectionally arranged [6, 9, 15–18] or in the form of woven fabric [19–22]. In addition to fibers, unidirectionally arranged [23] or woven [19, 23–26] thin flat tapes were also used as starting material structure for hot compaction.

Among above-mentioned materials, hot compacted PP was found to be the most promising candidate with potential for commercial development due to the fact that it can provide cost/performance balance for several applications [8]. It is now commercially available under the trade name of Curv® from Propex Fabrics. Regarding the structure of the preform, woven filaments or tapes were suggested to be the most useful structures because of the advantage of providing greater surface area [8]. This is important for sufficient contact and adhesion between layers.

The most critical processing parameter in hot compaction is the temperature. It determines the amount of matrix and the mechanical performance of the resultant composite. An optimum compaction temperature approximately ranges between onset and peak melting temperatures of the polymer. The major challenge here is to perform compaction in such a very narrow optimum window. In order to address this issue, Hine et al. [27] combined two techniques: hot compaction and film stacking. In order to use lower compaction temperature, they placed the films in between compacted preforms where the matrix material is mostly required. Thus, they did not only widen the processing temperature window but also improve the inter-layer strength. Overall, hot compaction technique can offer high modulus and strength thermoplastic composites with small loss of original fiber properties and provide strong fiber–matrix interface.

Another alternative method of making thermoplastic composite is using coextruded tapes. This technique was developed by Peijs et al. [12, 13] to produce all-PP composites. In their studies, two grades of PP with different melting temperatures were coextruded and then cold drawn to improve the mechanical properties. The coextruded tape composed of a highly oriented PP in the core and a copolymer PP in the skin. The temperature difference in the melting points of these two polymers allows melting the matrix component (skin) while keeping the reinforcement component (core) intact. Due to the several advantages that this technology presents: large processing temperature window (20–40 °C for PP), reduced risk of fiber orientation, and high fiber volume fraction (~90%), it was commercialized by Lankhorst-Indutech in the Netherlands under the trade name PURE® and also by its licensee Milliken in the USA under the trade name Tegris®.

Although coextrusion technique brings several advantages, incompatibility of two components used could lead to interface issue. Therefore, interface strength between

fiber and matrix could be lower for this type of composites compared to other all-polymer composites where an identical polymer is involved in both the fiber and matrix.

In a recent study, Zhang and Peijs [14] used bicomponent yarns instead of tapes. Unidirectionally aligned PET multifilament bicomponent yarns with core/sheath structure in which low melting temperature co-PET was used in the sheath, were consolidated by heat and pressure to obtain all-PET composite. They investigated the effects of consolidation temperature and pressure and found that the pressure values used had almost no impact on tensile properties. On the other hand, while longitudinal modulus and strength varies with temperature, transverse strength increases up to an optimum reached at a processing temperature of 220 °C. The examination of fracture surfaces revealed that tensile failure mode actually shifts from ductile to fragile when processing temperature was increased. It was attributed to an improvement in interfacial adhesion between matrix and fiber at comparatively higher consolidation temperature.

Nonwovens as preforms

Most of the above-mentioned studies on thermoplastic composite fabrication techniques were conducted on high performance fibers or highly oriented fibers and tapes. In addition, preforms were in the form of unidirectionally arranged filaments, tape, or woven fabric. In this study, we used bicomponent nonwoven fabrics with different polymer pairings and contents as a precursor to produce thermoplastic composites from conventional textile materials without using any resin or binder. The advantages of nonwoven fabrics for composites compared to other preforms are their low cost, high production rate, and convenience for randomization of fibers [2, 28]. For instance, even though a woven fabric with plain weave has maximum mechanical properties in the two perpendicular directions of fibers (0° and 90°), it has considerably lower mechanical properties in the diagonal and other directions [2]. In addition to the benefits that we gain from nonwovens, using the bicomponent structures in thermoplastic composite fabrication offers many advantages such as uniform distribution of matrix and excellent wetting.

We have examined the viability of a process which is similar to the co-extrusion approach proposed by Peijs et al. [12–14]. This process allows the production of composites directly from bicomponent nonwovens. Conceptually, the structure of the bicomponent fibers making up these nonwoven already mimics the fiber–matrix structure of fiber reinforced composites. The matrix polymer (sheath) usually has a lower melting point than the core or reinforced polymer, thereby if a temperature that is close to the melting temperature of the matrix is chosen,
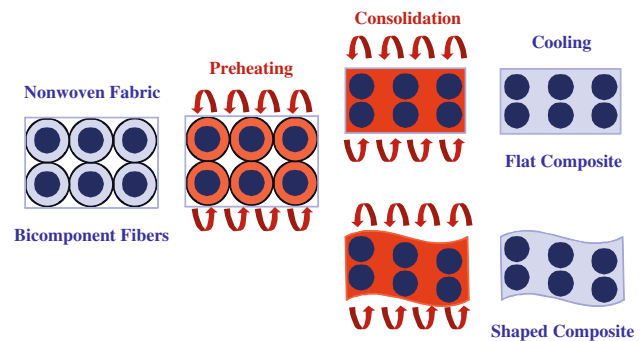

Fig. 1 Schematic representation of nonwoven composite making process

the applied heat to the preform will allow matrix polymer to soften. Afterward, by the means of pressure and heat, the matrix polymer flows and fills the inter-fibrillar spaces; therefore, consolidation can be achieved. On the other hand, the core polymer will retain its mechanical properties. Upon cooling, we can obtain either flat or shaped composites (or even be reshaped) depending on the type of mold used. This way, thermoplastic composites and laminates can be produced using only the bicomponent nonwoven webs or fabrics. Conceptual description of above-mentioned process is illustrated in Fig. 1. This process eliminates the need for any resin or binder usage and post-processing from composite production steps. The resultant composites are inexpensive and 100% thermoplastic, so that it is lightweight and reusable. Depending on the polymer combinations chosen, these novel nonwoven composites can combine the desired mechanical properties for many application areas. In this regard, one of the outcomes of this article is to establish what combination of mechanical properties these materials can offer.

Materials

Commercial fiber grades of PET, PA6, and PP were used as the core (reinforcement) polymer. Linear low density PE and PP were used as the sheath (matrix) polymer. Some of the basic properties and suppliers of these polymers are listed in Table 1.

Methods

Production of bicomponent fibers and nonwovens

Bicomponent nonwoven fibers and nonwovens were produced using the bicomponent spunbonding process (see Fig. 2) at the Nonwovens Cooperative Research Center's pilot facility (NC State University, Raleigh, NC, USA).

Table 1 Properties and suppliers of polymers

Polymer	Trade name	Supplier	Density[a], ρ (g/cm^3)	Melting temperature[b], T_m (°C)
PET	F-61HC	Eastman Chemical Co.	1.41	250
PA6	Ultramid BS-2702	BASF	1.13	220
PP	CP-360H	Sunoco	0.905	166
PE	Aspun 6850A	Dow Chemical Co.	0.955	129

[a] The density values of PA6, PP, and PE were obtained from corresponding polymer data sheet supplied by the producer. PET density value was taken from the reference [29]

[b] The melting temperatures of all polymers were peak melting temperatures and measured by means of a differential scanning calorimeter at a heating rate of 10 °C/min

The spunbonding process is a method of producing fabrics directly from polymers in a single step. It combines filament extrusion, drawing (attenuation), deposition, bonding, and winding (see Fig. 2). Therefore, it is one of the most cost-effective and fastest methods of making a fabric. As a comparison, the relative production rate ranges between 1 and 6 for weaving; 3 and 16 for knitting, whereas it is between 200 and 2,000 for spunbonding [31].

The bicomponent fiber cross-section chosen was a sheath–core structure (see Fig. 3) in which one component (core) is fully surrounded by the second component (sheath). Two polymer ratios used were 50 wt%/50 wt% and 75 wt%/25 wt% (core/sheath). Attenuated fiber samples which are continuous oriented filaments were collected before the deposition on the forming belt during the

Fig. 2 Schematic drawing of the bicomponent spunbonding process at NCSU [30]

Fig. 3 Sheath–core bicomponent fiber: **a** cross-section and **b** longitudinal view

process for investigation. Spunbond nonwoven fabrics with 250 g/m^2 basis weight were also produced using unheated calendaring rolls which can provide sufficient web integrity for handling at subsequent composite fabrication stages.

Fabrication of nonwoven composites

Nonwoven fabrics were cut to 20 cm × 20 cm dimensions. Single layer nonwoven fabrics were stacked on top of one another. Four different thicknesses were obtained using 2, 4, 8, and 16 layers of nonwoven fabrics. Each layer of these nonwoven fabrics had the dominant orientation in the machine direction. In order to get balanced structures, fiber orientation in these laminates was configured by simply rotating each layer with respect to its dominant orientation and placing it on top of the previous layer. A hot press was used to produce nonwoven composite. The cross-layered fabrics were then placed between Teflon® sheets to prevent fabrics from sticking on the hot surfaces of the press.

Direct composite fabrication from nonwoven fabrics comprises three stages: (i) preheating, (ii) compacting (consolidation), and (iii) cooling (see Fig. 1). In the first stage, the preform is heated to soften the matrix polymer under a comparatively low pressure (P_r) of 0.5 MPa. In this stage, residence time (t_r) and temperature (T_r) required for softening depend on the type of the matrix used and the thickness of the preform (see Table 2). In the second stage, the preheated preform is pressed between two heated plates and held for some time. Thus, matrix polymer flows and fills the gap between reinforcement fibers. At the same time, consolidation of the structure facilitates the removal of the unwanted voids that could weaken the resultant composite. In order to consolidate the structure, a high pressure (P_c) of 12 MPa was used. In this stage, consolidation time (t_c) and temperature (T_c) are variables that can affect the structure of the resultant composite. In the last stage, composite samples are quenched in between two metal plates at room temperature. Time–temperature and time–pressure profile during nonwoven composite fabrication can also be seen in Fig. 4. Solid line represents the change on the sample temperature, while the dotted line
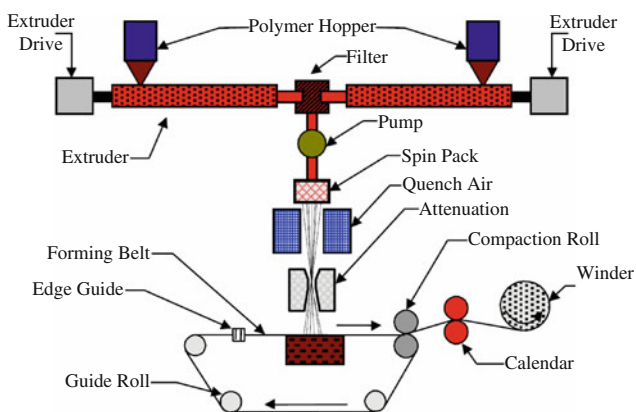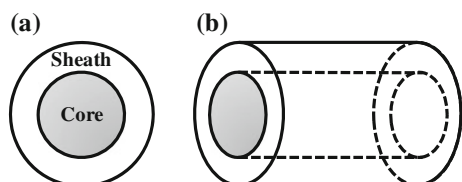
Table 2 Processing parameters

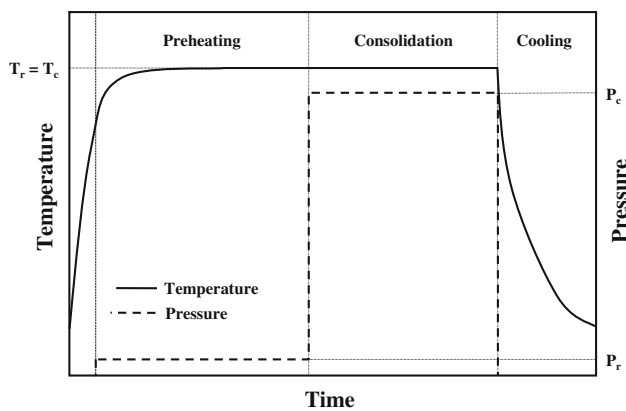| Processing parameters					
Matrix polymer	Number of layers	Residence temperature, T_r (°C)	Residence time, t_r (s)	Consolidation temperature, T_c (°C)	Consolidation Time, t_c (s)
PE	2	130	30	130	30
PE	4	130	60	130	60
PE	8	130	120	130	60
PE	16	130	240	130	90
PP	2	165	30	165	30
PP	4	165	60	165	60
PP	8	165	120	165	60
PP	16	165	240	165	90

Fig. 4 Time–temperature and time–pressure profile during nonwoven composite fabrication

shows the profile of the applied pressure on the sample. T_r and T_c were kept same for all samples, which makes the process flow easier in the hot press. The pressure was increased appreciably after the preheating stage to achieve a better consolidation.

Tensile testing of nonwoven composites

Composite tensile testing was performed to determine the tensile strength of the composites formed with 2, 4, and 8 plies of nonwoven fabrics. Slippage in the grips was prevented using diamond grip faces, while the sample fracture at the grip was prevented using dog bone-shaped specimens as specified in the ASTM Standard D 638-08. MTS Q-Test machine with 90 kN load cell was used for the test. The crosshead speed was adjusted to 51 mm/min. Mechanical parameters: initial modulus, tensile strength, strain at break, and tensile energy to break were measured.

Izod impact testing

The notched izod impact test specimens were machined from a nonwoven composite sample which was made from

16 plies of nonwoven fabrics and had around 4 mm thickness. Six specimens were prepared for each sample and conditioned 48 h before the test. Samples were tested in the Tinius Olsen Model 92T impact testing machine according to the ASTM Standard D256-06 Method A. Testing conditions were reported as 23 °C and 50% relative humidity. All specimens have a dimension of 12.7 ± 0.2 mm × 63.5 ± 2 mm and a notch depth of 2 ± 0.2 mm. Impact strength and impact resistance values were noted and averaged for each sample.

Wide angle X-ray

An Omni instrumental wide angle X-ray diffractometer (WAXD) was used to determine the crystallite dimensions for each of the components in the bicomponent nonwoven fibers and composites. The instrument was operated at 30 kV and 20 mA with a Be-filtered CuKα radiation source ($\lambda = 1.54$ Å). The fibers were manually wound around a sample holder which was then perpendicularly positioned to the X-ray beam. They were scanned at a rate of 0.1 s^{-1} from 5° to 40° (2θ). The nonwoven composite specimens were mounted onto the sample holder. They were scanned at a rate of 0.05 s^{-1} from 10° to 40°.

Differential scanning calorimetry (DSC)

Thermal analysis was carried out for bicomponent fibers and nonwoven composites by means of differential scanning calorimetry (DSC). Perkin Elmer Diamond DSC calorimeter and Pyriss Series Diamond DSC software were used for the thermal analysis of all the samples. The samples weighed between 3 and 5 mg. The samples were scanned at the heating rate of 10 °C/min in the temperature range from 25 to 270 °C.

Scanning electron microscopy (SEM)

Scanning electron microscope (SEM) images were taken for nonwoven composites. In order to take a clear

cross-section image, samples were embedded into liquid nitrogen in which they freeze, and then fractured using a razor blade. SEM analysis was performed on the samples after they were coated with a layer of AuPd at a 5 kV accelerating voltage and 40 nA beam current in a Hitachi S-3200 SEM.

Results and discussions

Microstructural analysis

Effect of processing temperature

Processing temperature is one of the most important parameters that can affect the final composite microstructure. In order to investigate the effect of temperature, we used series of temperatures ranging from 125 to 150 °C with increments of 5 °C for PE matrix samples. In the case of processing at 125 °C which is slightly lower than the peak melting temperature of the PE component (127 °C) in the fiber, the matrix polymer did not melt enough to flow and fill the gaps in the composite structure. This situation is depicted in Fig. 5a. It was shown that insufficient heat could cause defects such as voids in the structure and delamination easily occurs for this structure due to the lack of adhesion between layers. On the other hand, processing at temperatures equal or greater than 135 °C led to oversoftening the molten matrix polymer. Combined with the effect of high pressure, the molten polymer was squeezed out from structure; and therefore, the composite structure lost its integrity (see Fig. 5b). When 130 °C (±2 °C) was used, the molten matrix polymer was able to reach a melt viscosity level allowing the polymer to flow and fill the interstices between fibers (see Fig. 6). Thus, a composite structure with fewer defects could be produced.

Effect of reinforcement volume fraction

Reinforcement volume fraction determines the packing density of the composite. In most practical applications, a higher reinforcement volume fraction is desired. However, some limitations exist due to the distribution of the fibers in the structure. A random fiber distribution reduces the possible reinforcement volume fraction values. PA6/PE nonwoven composite with high reinforcement volume fraction ratio of 0.72 (achieved at polymer weight ratio of 75/25) is shown in Fig. 7. When this structure was examined, some matrix-free regions were observed. This is mainly due to the random fiber orientation in nonwoven structures, which does not allow close packing. On the other hand, when the reinforcement volume fraction was reduced to values between 0.4 and 0.5 (achieved at polymer ratio of 50/50), nonwoven composites could be produced with far fewer defects in the structure. Some examples of these composites are shown in Fig. 8.

Characterization of bicomponent fibers and nonwoven composites

Thermal properties

In order to show process–structure relationship, thermal analysis was carried out. Melting and crystallization temperatures for bicomponent fibers and composites were determined by analyzing DSC traces for both bicomponent fibers and nonwoven composites made thereof and listed in Table 3. These results were obtained from the first melting endotherms and cooling exotherms. It is important to point out that these results include the thermal history of the material being tested. Results show that the melting temperatures of both sheath and core polymers increased after going through the composite fabrication process. The
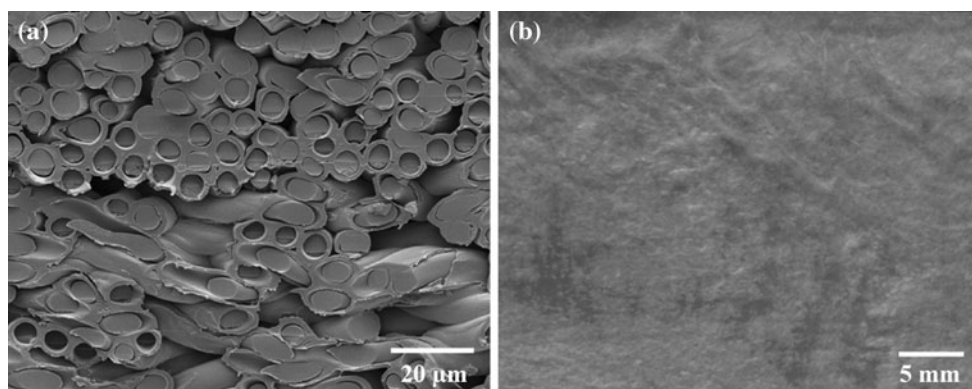

Fig. 5 PP/PE (50 wt%/50 wt%) nonwoven composites processed at **a** 125 °C and **b** 135 °C
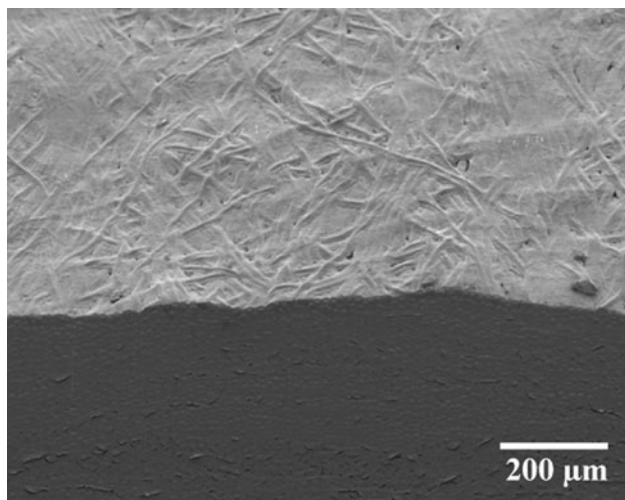
Fig. 6 SEM picture of PA6/PE (50 wt%/50 wt%) nonwoven composite processed at 130 °C

increase in the melting points of the polymers can be explained by means of the Gibbs free energy theory (Eq. 1). According to this theory, the change in the Gibbs free energy (ΔG) per unit mass upon melting is zero. Hence, the melting temperature (T_m) is the ratio of the change of enthalpy (ΔH) to entropy (ΔS) from the crystalline state to the melt (Eq. 2).

$$\Delta G = \Delta H - T\Delta S \tag{1}$$

$$T_m = \Delta H / \Delta S \tag{2}$$

Based on this theory, it is possible to increase the melting point of a polymer by changing ΔH or ΔS of the system. For polymer systems, ΔH is determined by the specific interactions between polymer chains. It can be affected by the degree of the chain regularity, perfection of the crystals, and size of the crystallites. During nonwoven composite fabrication process, sheath component in the bicomponent fiber underwent partial or complete melting with the loss of the microstructure associated with it. After partial or complete melting of the initial lamellae, new lamellae were formed during recrystallization. Owing to the long consolidation time, high temperature and pressure, an annealing effect can be achieved. Thus, the thickness of the new lamellae became larger than that of initial lamellae [32]. This leads to an increase in the enthalpy required to melt crystallites; and therefore, an increase in the melting point of the sheath polymer was observed.

In addition to an increase in the ΔH, a reduction in the ΔS which is determined by the orientational and conformational entropies of polymer chains could be observed for polymeric materials heated under constrained conditions [33]. Typically, polymers will try to relax by restoring their preferential isotropic structure, when they are heated. This leads to a transition to more disordered phase with an increase in the entropy. However, it is possible to avoid this relaxation by heating and melting polymers under constrained condition. Thus, polymer chains will have very limited freedom to switch to more disordered phase. During preheating and consolidation stages, bicomponent fibers were constrained between hot plates under high pressure, and therefore, polymer chains in sheath polymer were prevented from any structural relaxation. At the same time, a melt orientation was introduced. Therefore, a reduction in the orientational and conformational entropies of polymer chains which could cause an increase in the melting point of sheath polymer was achieved. Similarly, the melting temperature shifts for constrained fibers were also reported in the literature [14, 17, 33].

Figure 9 presents the DSC endotherms of bicomponent fibers and nonwoven composites. In this figure, dark curves show the DSC endotherms of nonwoven composites while the lighter curves show those of bicomponent fibers. In each curve, there are two melting endotherms where the melting endotherms at higher temperatures belong to core or reinforcement polymers. For example, PA6/PP bicomponent fiber showed two melting endotherms at 166 and
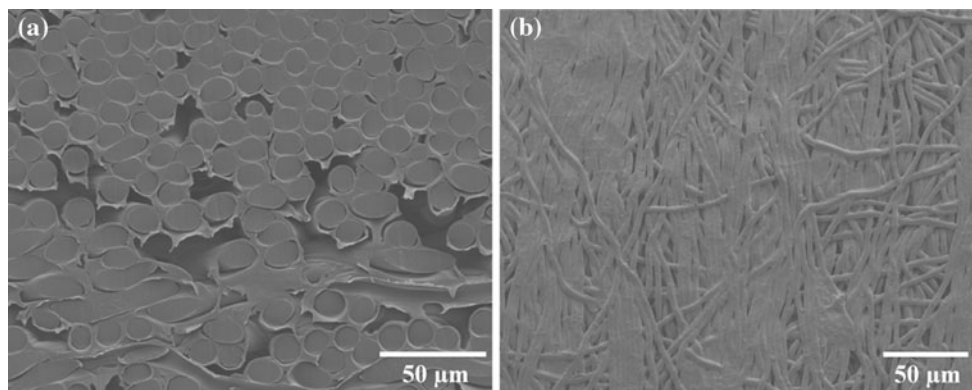

Fig. 7 SEM pictures of PA6/PE (75 wt%/25 wt%) nonwoven composite processed at 129 °C with a fiber volume fraction ratio of 0.72: a cross-section, b surface
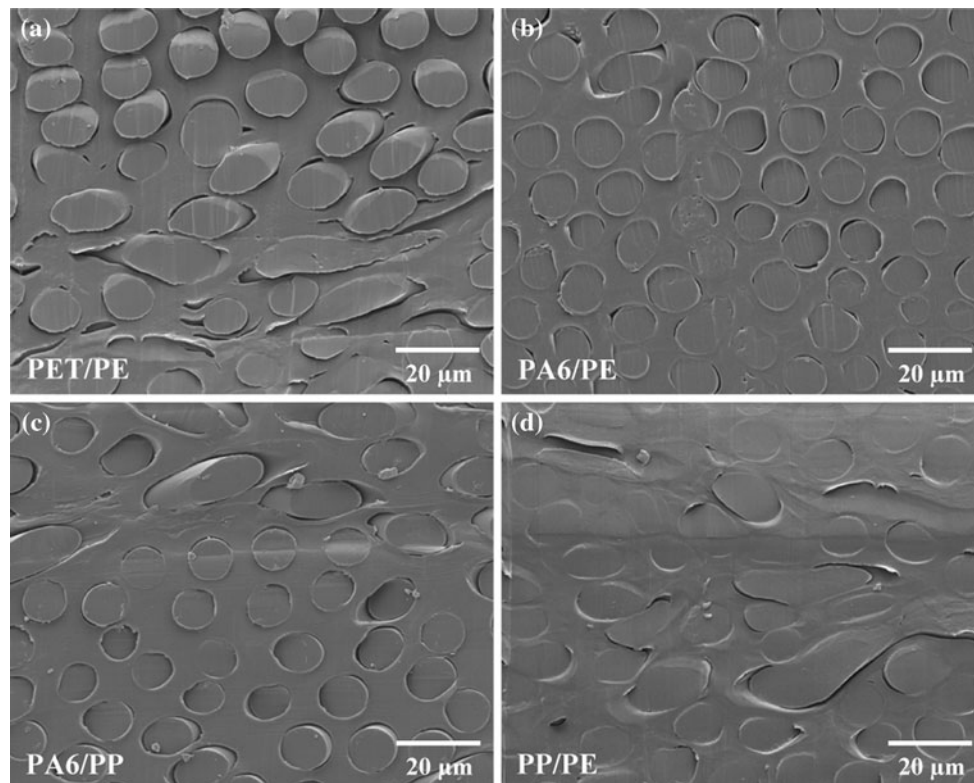
Fig. 8 SEM pictures of nonwoven composites with a fiber volume fraction ratio of **a** 0.40 (PET/PE, made at 128 °C), **b** 0.46 (PA6/PE, made at 129 °C), **c** 0.44 (PA6/PP, made at 164 °C), and **d** 0.51 (PP/PE, made at 130 °C)

Table 3 Melting and crystallization temperatures of bicomponent fibers and nonwoven composites

Polymers Core/sheath	Bicomponent fiber				Nonwoven composite			
	Core		Sheath		Fiber		Matrix	
	T_m (°C)	T_c (°C)	T_m (°C)	T_c (°C)	T_m (°C)	T_c (°C)	T_m (°C)	T_c (°C)
PET/PE	250	206	128	117	255	206	130	116
PA6/PE	216	191	127	118	225	191	130	115
PA6/PP	216	189	166	119	222	189	172	116
PP/PE	162	122	128	117	166	120	132	116

216 °C in which the later belongs to PA6 (core) polymer. When the melting behaviors of the core polymers were analyzed, two consecutive endothermal melting peaks were observed. For instance, PA6 component in PA6/PP fiber had two consecutive peaks at 216 and 222 °C. In this type of broad endotherm for a core polymer, the lower temperature melting peak corresponds to crystallites with imperfections while the higher temperature melting peak represents the more perfect crystallites. It was found that for bicomponent fibers, the lower temperature melting peaks were more dominant than the higher one. However, after composite fabrication process, the intensity of the lower temperature melting peak reduced substantially with an increase in the intensity of the higher temperature

melting peak. This indicates that the distribution of crystal sizes was narrowed and imperfections in the former crystallites were reduced during composite fabrication. It can be attributed to the annealing effect brought by the composite fabrication. Therefore, the melting temperatures of the core polymers shift to higher temperatures after formation of the composite.

Contrary to melting temperature, a change in crystallization temperature was not observed for core polymers except PP. However, there is a slight decrease in the crystallization temperatures of sheath polymers. When we compare cooling behavior of sheath polymer in the fiber with that of matrix polymer, it can be expected from sheath polymer to cool faster during fiber formation than the
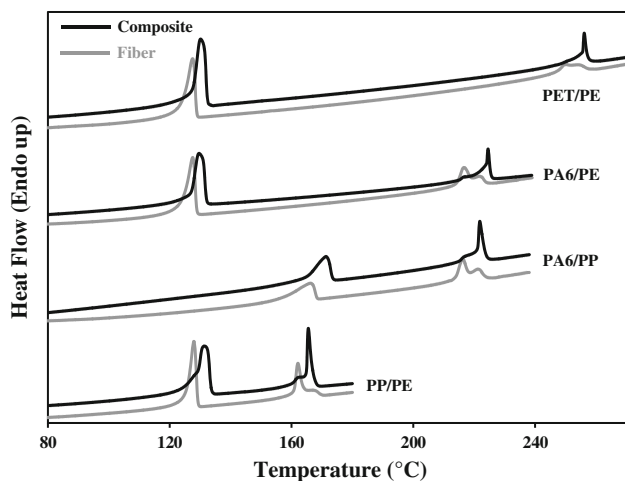
Fig. 9 DSC endotherms of bicomponent fibers and nonwoven composites

formation of matrix phase in composite. This is due to the fact that fibers have larger surface area to volume ratio than composites. Therefore, they can crystallize at higher temperatures compared to bulk matrix material in the composite. For PP/PE nonwoven composites, this situation is more complicated because these polymers have close crystallization temperatures. For this reason, any change attributed by heat treatment could affect the behavior of the second component.

Crystallinity and crystalline structure

The degree of crystallinity of each polymer in the bicomponent fibers and composites was calculated using Eq. 3 [34]:

$$X = \frac{\Delta H_f - \Delta H_c}{w \times \Delta H_f^o} \qquad (3)$$

where X is the degree of crystallinity of a material; ΔH_f is the heat of fusion of a polymer (measured from area under melting peak curve of DSC); ΔH_c is the heat of cold crystallization of the polymer; ΔH_f^0 is the theoretical heat of fusion for perfectly crystalline polymer (obtained from literature); and w is the weight fraction of the polymer in bicomponent or composite structure.

The theoretical heats of fusion for homopolymers were assumed to be 230 J/g [35], 293 J/g [35], 140 J/g [36], and 209 J/g [37] for PA6, PE, PET, and PP, respectively. Cold crystallization peak was not observed for polymers in both bicomponent fibers and composites. Results from the degree of crystallinity calculation are shown in Table 4. A significant increase in the crystallinity values of sheath polymer was observed for all polymer pairs when they were converted to the composite.

The crystalline structures for bicomponent fibers and nonwoven composites were examined using X-ray diffractions (see Fig. 10 and Table 5). General trend for matrix polymers is more sharpened and better resolved peaks. For instance, the intensity of reflections at angular position 2θ of 22° which corresponds to 110 plane of PE increased appreciably for composite samples. It suggests that size and/or perfection of crystallites that is perpendicular to this plane increased. Moreover, reflections around angular position 2θ of 25° corresponding to 200 plane of PE appeared for composite samples suggesting a crystal growth in the direction perpendicular to this plane. Similarly, characteristic peaks for PP matrix in PA6/PP at 15° (110), 17.8° (040), and 19.4° (130) also showed up for composite samples indicating a crystal growth.

Crystal sizes for PET/PE and PP/PE samples were also calculated using Scherrer formula (Eq. 4) and summarized in Table 6. Results clearly show that crystal sizes (thickness of the lamellae) of PE have considerably improved during composite fabrication. This explains why significant increases in the crystallinity values of sheath polymers were obtained.

$$w = \frac{0.94 \times \lambda}{\beta \times \cos \theta} \qquad (4)$$

where w is the width of crystallite (Å); λ is the wave-length (Å) (Cu Kα (λ = 1.54 Å) was used); β is the full width at half maximum intensity (radians); and θ is the Bragg's angle (radians).

Overlay of diffraction patterns for PP/PE samples also revealed a slight shift in the diffraction peak positions to higher angles accompanied by increased peak intensity. It suggests that location of the lattice plane changed and unit cell distance (d-spacing) became smaller. It can be

Table 4 Degree of crystallinity values for bicomponent fibers and nonwoven composites

Polymers	Bicomponent fiber		Nonwoven composite	
Core/sheath	Core X_c	Sheath X_s	Fiber X_f	Matrix X_m
PET/PE	0.332	0.473	0.374	0.670
PA6/PE	0.290	0.467	0.285	0.598
PA6/PP	0.309	0.395	0.294	0.478
PP/PE	0.417	0.518	0.449	0.640
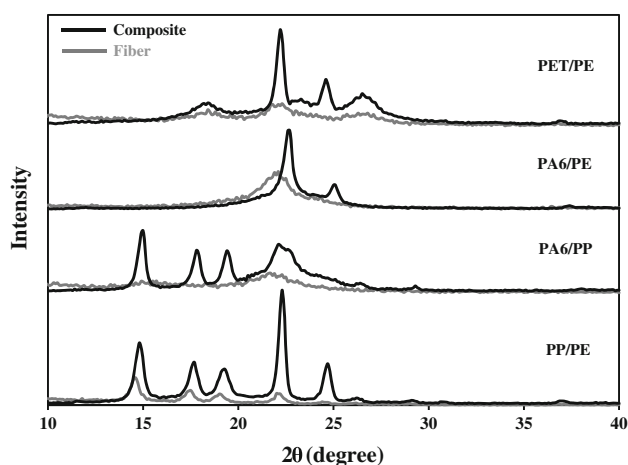
Fig. 10 WAXD patterns for bicomponent fibers and nonwoven composites

Table 6 Crystal sizes of PE in plane (110) for PET/PE and PP/PE

Polymer	Sample	2θ (°)	Crystal width (Å)
PET/PE	Fiber	22.3	45
PET/PE	Composite	22.2	167
PP/PE	Fiber	22.0	123
PP/PE	Composite	22.3	212

attributed to the combination of high pressure and annealing effects on the crystal structures. At the same time crystallite sizes increased so that crystallinity of PP component in the PP/PE composite increased from 41.7 to 44.9%.

We also observed an increase in the crystallinity of PET component in PET/PE samples after composite fabrication. When the X-ray diffraction patterns of these samples were investigated, better resolved peaks for PET at 18.4° (010) and 26.5° (100) in composite sample were obtained. It indicates that the processing temperature of 128 °C accompanied with high pressure induced an improvement on crystal size distribution and perfections. On the other hand, although the degree of crystallinity for PA6 did not undergo appreciable change after the formation of composites, an intensity increase with better resolved peak at 22.1° (200) in PA6/PP composite sample suggests a crystal perfection effect brought about by annealing.

Mechanical properties

Comparison of tensile and impact properties

One of the important outcomes of this study was to evaluate the mechanical properties (tensile and impact) of nonwoven composites and establish how the mechanical properties

compared to other conventional and widely used thermoplastic composites such as glass fiber reinforced thermoplastic composites. Therefore, tensile and impact properties of nonwoven composites were measured and compared with a glass mat reinforced polypropylene thermoplastic composite (GMT) having 40% reinforcement glass fiber which can be comparable to the reinforcement fiber percentages (40–51%) of nonwoven composites. Another reason for choosing this structure is the fact that glass fiber mat is one of the closest structure to the bicomponent nonwoven preform in terms of fiber orientation. In this regard, Table 7 summarizes results obtained for nonwoven composites and compares with GMT composite. Results showed that in general nonwoven composites yielded higher specific strength values up to 97 MPa/g cm^{-3} obtained for PA6/PE nonwoven composite. Thus, nonwoven composites except PP/PE nonwoven composite outperform the GMT in terms of specific stress. One of the other outstanding performances of nonwoven composites compared to GMT composite in terms of the tensile properties is the high strain at break values. Especially, PP/PE nonwoven composites showed tremendous strain at break value of 152% with a standard deviation (σ) of 8%, and therefore, they were able to absorb high tensile energy (65 MJ/m^3, $\sigma = 5$).

Notched izod impact strength values of nonwoven composites and GMT composite are also presented in Table 7. All nonwoven composite samples showed non-break type of failure described in ASTM standard D256. Among the tested composite samples, PA6/PP nonwoven composite performed best with an average value of 147 kJ/m^2 ($\sigma = 6$). This value is almost 15 times higher than that of GMT composite. High impact strength values observed for all nonwoven composites suggest that they can be a good candidate for applications where high impact energy absorption is required.

Table 5 Observed peak positions for each polymer in bicomponent fibers and nonwoven composites

Polymer	1st Peak position		2nd Peak position		3rd Peak position	
	2θ (°)	Crystallographic plane (hkl)	2θ (°)	Crystallographic plane (hkl)	2θ (°)	Crystallographic plane (hkl)
PET	18.4	(010)	26.3–26.5	(100)	–	–
PA6	21.7–22.1	(200)	–	–	–	–
PP	14.6–15	(110)	17.5–17.8	(040)	19–19.4	(130)
PE	22–22.3	(110)	24.6–25	(200)	37.1–37.4	(020)

Table 7 Comparison of mechanical properties of thermoplastic composites

	PET/PE	PA6/PE	PA6/PP	PP/PE	GMT[a]	Curv[®b]	Pure[®c]
Reinforcement component (%)	40	46	44	51	40	78	90
Overall density (g/cm^3)	1.14	1.04	1.01	0.93	1.19	0.93	0.77
Tensile modulus (GPa)	2.2	1.7	1.6	1.5	5.8	3.0	1.5–13
Specific modulus (GPa/g/cm^{-3})	1.9	1.6	1.6	1.6	4.9	3.2	1.9–17
Tensile strength (MPa)	83	100	73	52	77	60	4.5–385
Specific strength (MPa/g/cm^{-3})	73	97	72	56	65	64	5.8–500
Strain at break (%)	68	86	71	152	4	27	1–7
Tensile energy to break (MJ/m^3)	41	55	34	65	–	–	–
Notched izod impact test (kJ/m^2)	76	133	147	48	10	–	–

[a] Glass mat reinforced thermoplastic PP composite [38]

[b] Hot compacted woven PP tape thermoplastic composite [18, 19]

[c] Coextruded unidirectional PP tape thermoplastic composite [13]

Although nonwoven composites offered higher specific strength (except PP/PE nonwoven composite), strain at break and impact strength compared to GMT, they showed lower tensile modulus values. Results showed that the highest tensile modulus of 2.2 GPa ($\sigma = 0.3$ GPa) was obtained for the PET/PE nonwoven composite. This value is almost two times lower than that of GMT composite (4.9 GPa). It is due to the fact that glass fiber is a high stiffness fiber compared to conventionally produced thermoplastic textile fibers.

In order to give a broad perspective to readers, we also compared nonwoven composites with two new all-polymer composites (Curv® and Pure®) in Table 7. However, it is important to point out that these all-polymer composites do not have comparable reinforcement fiber percentages (78% for Curv® [19] and 90% for Pure® [13]) and preform structures with nonwoven composites (<51%). As an example to Curv®, a hot compacted woven (plain) PP tape thermoplastic composite [18, 19] was chosen. Since only unidirectionally arranged structure exists for Pure® Technology in the current literature, we present coextruded unidirectional PP tape thermoplastic composite properties [13] in Table 7. When mechanical properties are compared, nonwoven composites yielded comparable or higher specific strength and strain at break than Curv® and Pure® (except the longitudinal specific strength of Pure®). On the other hand, they generally showed lower specific modulus. It is due to the fact that reinforcement tapes in two all-polymer composites are highly oriented structures compared to bicomponent fibers. At the same time the reinforcement component percentages for these two all-polymer composites are higher than nonwoven composites.

One of the important parameter that could have negatively affected the mechanical responses of nonwoven composites is the fiber–matrix interface. When we investigate the micro-structure of nonwoven composites (see

Fig. 8), noticeable fiber–matrix debonding for PET/PE, PA6/PP, and PA6/PE can be observed. This debonding issue could lead to weak fiber–matrix strength and lower the mechanical properties. The question remains whether it is possible to improve interface and obtain even stronger nonwoven composites by modifying the process and using some interface compatibilization agents. This part of the study is out of the scope of this article and will be addressed in a subsequent article.

Effect of number of layers (Lamina) on tensile properties

Nonwoven composites composed of 2, 4, and 8 layers of nonwoven fabrics with each having 250 g/m^2 basis weight were produced to determine the effect of number of layers on tensile properties of the composites. In this regard, the tensile properties of nonwoven composites with varying number of layers are presented in Figs. 11 and 12. Results shown in Fig. 11 indicate that there is no difference between the tensile strength values of composites having different number of layers. Similarly, as the number of layers in the composites increase, the strain value for the composite does not change
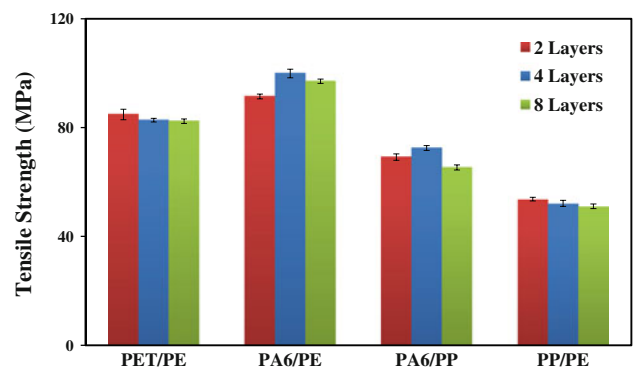

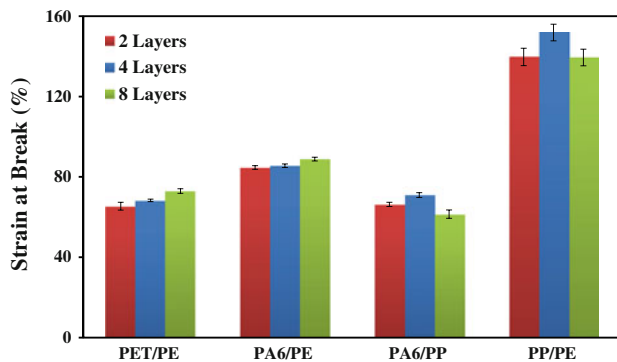**Fig. 11** Tensile strength values of nonwoven composites

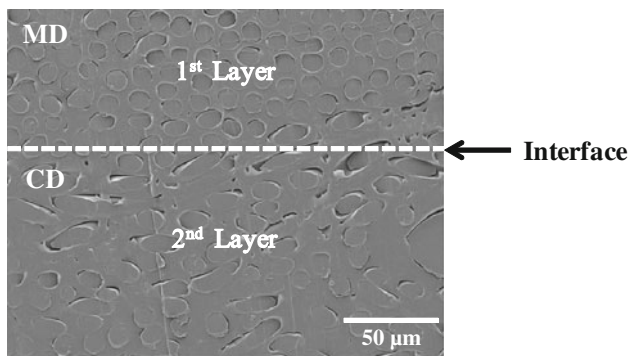**Fig. 12** Strain at break values of nonwoven composites

Fig. 13 Interface in between layers of PA6/PE composite

(see Fig 12). These results suggest that tensile properties of the nonwoven composites are not dependent on the thickness of the composites studied.

The interface in between layers was also investigated by morphological analysis. In order to find the location where two layers came into contact, preferred fiber distributions in the cross-section of nonwoven composite were tracked. Since cross-layering of nonwoven fabrics during composite fabrication enables to get two preferential directions of fiber distribution: along the production direction of nonwoven fabric known as machine direction (MD) and across the width of the fabric which is cross-direction (CD). Thus, we were able to determine the intersection of two layers during morphological examination. One of the examples of this is illustrated in Fig. 13 which shows the cross-sectional SEM image of a PA6/PE nonwoven composite. From this image, it is clearly seen that there is a smooth transition from one layer to another layer without any matrix-free region indicating an intact composite structure.

Conclusions

In this study, we introduced a new technique to produce engineering thermoplastic composites from bicomponent

nonwovens without using any additional resin or binder. Inherent composite structure of the bicomponent fibers enabled to obtain fiber reinforced thermoplastic composites in which PET, PA6, and PP were the reinforcement while PP and PE were the matrix. The effects of temperature and fiber volume fraction on the structure of nonwoven composites were studied using microstructural analysis. Processing temperatures of 130 °C for PE matrix and 165 °C for PP matrix were found to be the most favorable conditions for producing nonwoven composites with the fewer amount of defects under high pressure. Combination of two factors: (i) random distribution of the fibers and (ii) cross-layering limited to achieve high reinforcement volume fraction (e.g., $f = 0.72$ for PA6/PE) in the resultant composite. However, nonwoven composites (PET/PE, PA6/PE, PA6/PP, and PP/PE) with $f \leq 0.51$ were successfully produced.

In order to provide a better insight for the process–structure relationship, thermal properties, crystallinity, and crystal structure of bicomponent nonwovens and nonwoven composites were analyzed and compared. Our findings showed that the melting temperature and degree of crystallinity of sheath polymers increased when they became matrix. This was attributed to the annealing and constrained fiber effects brought by composite processing. A significant increase in the crystallite sizes for matrix phase achieved after composite fabrication also supports our conclusion. We also observed melting temperature rises for reinforcement fibers. This was also explained to be a result of thermal treatment under pressure which could lead to a better distribution of the crystallite sizes and improved perfections of crystallites.

Mechanical performance of nonwoven composites were also reported and compared with a GMT composite which has a polypropylene matrix and 40% glass fiber content. In general, nonwoven composites showed lower specific modulus but higher specific stress than GMT composite. On the other hand, they provided superior strain at break (68–152%) and impact strength (48–147 kJ/m^2) values compared to GMT composite (4% and 10 kJ/m^2, respectively).

Nonwoven composites with different thicknesses achieved with cross-layering 2, 4, and 8 plies of nonwovens having 250 g/m^2 were also compared in terms of their mechanical (tensile) performance. Our findings showed that tensile properties are not affected by the number of plies in the composite. Moreover, morphological analysis of the intersection of two layers revealed an intact composite structure without any separation or matrix-free region at the interface.

In conclusion, this study shows that thermoplastic nonwoven composites with random fiber distribution can be produced using only bicomponent nonwovens as a

precursor. The resultant composites have isotropic structure with uniform distribution of matrix and high fiber volume fraction at the same level of fiber orientation. From an industrial point of view this technique permits the transformation of an inexpensive preform into an engineered thermoplastic composite in one step with excellent wetting characteristics of matrix polymer.

References

1. Gamstedt EK, Berglund LA (2003) In: Harris B (ed) Fatigue in composites: science and technology of the fatigue response of fibre-reinforced plastics. CRC Press, Boca Raton, FL
2. Shanks RA (2004) In: Baillie C (ed) Green composites: polymer composites and the environment. Woodhead Pub, Abington, Cambridge
3. Capiati NJ, Porter RS (1975) J Mater Sci 10:1671. doi:10.1007/BF00554928
4. He T, Porter RS (1988) J Appl Polym Sci 35:1945
5. Zhang JM, Reynolds CT, Peijs T (2009) Compos Part A: Appl Sci Manuf 40:1747
6. Hine PJ, Ward IM, Olley RH, Bassett DC (1993) J Mater Sci 28:316. doi:10.1007/BF00357801
7. Ward IM, Hine PJ (1997) Polym Eng Sci 37:1809
8. Ward IM, Hine PJ (2004) Polym 45:1413
9. Yan R, Hine P, Ward I, Olley R, Bassett D (1997) J Mater Sci 32:4821. doi:10.1023/A:1018647401619
10. Lacroix F, Werwer M, Schulte K (1998) Compos Part A: Appl Sci and Manuf 29:371
11. Lacroix F, Lu H-Q, Schulte K (1999) Compos Part A: Appl Sci and Manuf 30:369
12. Peijs T (2003) Mater Today 6:30
13. Alcock B, Cabrera NO, Barkoula N, Loos J, Peijs T (2006) Compos Part A: Appl Sci and Manuf 37:716
14. Zhang JM, Peijs T (2010) Compos Part A: Appl Sci and Manuf 41:964
15. Olley RH, Bassett DC, Hine PJ, Ward IM (1993) J Mater Sci 28:1107. doi:10.1007/BF00400899
16. Kabeel MA, Bassett DC, Olley RH, Hine PJ, Ward IM (1994) J Mater Sci 29:4694. doi:10.1007/BF00356511
17. Rasburn J, Hine PJ, Ward IM, Olley RH, Bassett DC, Kabeel MA (1995) J Mater Sci 30:615. doi:10.1007/BF00356319
18. Abo El-Maaty MI, Bassett DC, Olley RH, Hine PJ, Ward IM (1996) J Mater Sci 31:1157. doi:10.1007/BF00353094
19. Hine PJ, Ward IM, Jordan ND, Olley R, Bassett DC (2003) Polymer 44:1117
20. Jordan ND, Bassett DC, Olley RH, Hine PJ, Ward IM (2003) Polymer 44:1133
21. Hine PJ, Ward IM (2006) J Appl Polym Sci 101:991
22. Hine PJ, Ward IM, Maaty MIAE, Olley RH, Bassett DC (2000) J Mater Sci 35:5091. doi:10.1023/A:1004835816735
23. Jordan ND, Olley RH, Bassett DC, Hine PJ, Ward IM (2002) Polymer 43:3397
24. Hine PJ, Ward M, Teckoe J (1998) J Mater Sci 33:2725. doi:10.1023/A:1017540530295
25. Teckoe J, Olley RH, Bassett DC, Hine PJ, Ward IM (1999) J Mater Sci 34:2065. doi:10.1023/A:1004555608836
26. Amornsakchai T, Bassett DC, Olley RH, Hine PJ, Ward IM (2000) J Appl Polym Sci 78:787
27. Hine PJ, Olley RH, Ward IM (2008) Compos Sci Technol 68:1413
28. Reid RL (1998) Structural mechanics of textile composites: effect of braid construction and geometric parameters on composite performance. PhD dissertation, North Carolina State University, Raleigh, NC
29. Iroh JO (1999) In: Mark JE (ed) Polymer data handbook. Oxford University Press, New York
30. Fedorova N (2006) Investigation of the utility of islands-in-the-sea bicomponent fiber technology in the spunbond process. PhD dissertation, North Carolina State University, Raleigh, NC
31. Jirsâk O, Wadsworth LC (1999) Nonwoven textiles. Carolina Academic Press, Durham, NC
32. Bershteæin VA, Egorov VM (1994) Differential scanning calorimetry of polymers: physics, chemistry, analysis, technology. Ellis Horwood, New York
33. Barkoula N, Peijs T, Schimanski T, Loos J (2005) Polym Compos 26:114
34. Choi YB, Kim SY (1999) J Appl Polym Sci 74:2083
35. Wunderlich B (1973) Macromolecular physics. Academic Press, New York
36. Mehta A, Gaur U, Wunderlich B (1978) J Polym Sci: Polym Phys Ed 16:289
37. Clark EJ, Hoffman JD (1984) Macromolecules 17:878
38. Biron M (2007) Thermoplastics and thermoplastic composites: technical information for plastics users. Elsevier, Oxford